Article

pubs.acs.org/Biomac

Thermoresponsive Bacterial Cellulose Whisker/Poly(NIPAM-*co*-BMA) Nanogel Complexes: Synthesis, Characterization, and Biological Evaluation

Lei Wu,[†] Hui Zhou,[†] Hao-Jan Sun,[‡] Yanbing Zhao,[†] Xiangliang Yang,[†] Stephen Z. D. Cheng,[‡] and Guang Yang*[,†]

[†]National Engineering Research Center for Nano-Medicine, College of Life Science and Technology, Huazhong University of Science and Technology, Wuhan, 430074, China

[‡]College of Polymer Science and Polymer Engineering, The University of Akron, Akron, Ohio 44325, United States

ABSTRACT: Dispersions of poly(*N*-isopropylacrylamide-*co*-butyl methacrylate) (PNB) nanogels are known to exhibit reversible thermosensitive sol−gel phase behavior and can consequently be used in a wide range of biomedical applications. However, some dissatisfactory mechanical properties of PNB nanogels can limit their applications. In this paper, bacterial cellulose (BC) whiskers were first prepared by sulfuric acid hydrolysis and then nanosized by high-pressure homogenization for subsequent use in the preparation of BC whisker/PNB nanogel complexes (designated as BC/PNB). The mechanical properties of PNB was successfully enhanced, resulting in good biosafety. The BC/PNB nanogel dispersions exhibited phase transitions from swollen gel to shrunken gel with increasing temperature. In addition, differential scanning calorimetry (DSC) data showed that the thermosensitivity of PNB nanogels was retained. Rheological tests also indicated that BC/PNB nanogel complexes had stronger gel strengths when compared with PNB nanogels. The concentrated dispersions showed shear thinning behavior and improved toughness, both of which can play a key role in the medical applications of nanogel complexes. Furthermore, the BC/PNB nanogel complexes were noncytotoxic according to cytotoxicity and hemolysis tests. Concentrated BC/PNB nanogel dispersion displayed gel a forming capacity in situ by catheter injection, which indicates potential for a wide range of medical applications.

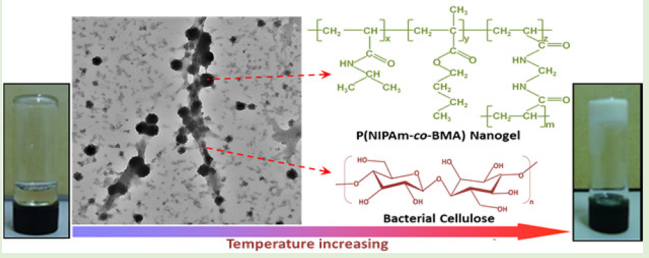

INTRODUCTION

Nanogels are cross-linked polymer gels, usually occurring as well-dispersed nanoparticles in aqueous media.[1] Nanogel particles have an average diameter in the range of 1−1000 nm. They may possess high environmental sensitivity, with heightened response to changes in temperature, pH, light, chemical stimuli, etc. Poly(*N*-isopropylacrylamide) (PNIPAM) nanogels are thus by far the most thoroughly investigated thermosensitive nanogels.[2] They are known to demonstrate dehydrating and shrinking behaviors and a reversible volume transition in water at a temperature around 32 °C, known as its lower critical solution temperature (LCST).[3−5] This indicates that aqueous dispersions of PNIPAM nanogels can form macroscopic gels *in situ* after being injected into human body. Therefore, various nanostructured PNIPAM materials are of great interest in biomedical applications for applications such as drug and gene carriers.[6−8] Other applications include sensors,[9] switching surfaces, adhesives,[10] temperature-targeted therapy materials,[11,12] and tissue-engineering materials.[13,14]

Cellulose is the most abundant natural biological polymer. In addition to plant cellulose, some bacteria such as *Acetobacte xylinum* (Ax) can also synthesize cellulose, and this kind of cellulose is generally called BC. This material possesses a range of unique and desirable properties such as high crystallinity,[15] high water holding capacity,[16] excellent mechanical[17] and thermal properties,[18] biodegradability and biocompatibility, and potential for preparation by controllable biosynthesis.[19] Nanocrystalline cellulose (NCC), also known as whiskers, consist of rod-like cellulose crystals with width of 5−70 nm and length ranging from 100 nm to several micrometers.[20] They are prepared by removal of amorphous portions from purified cellulose by acid hydrolysis, often followed by ultrasonic treatment. The commercialization of cellulose nanocrystals is still at an early stage but appears very promising due to its strengthening effect and optical properties.[21−24] NCC has been found useful in areas such as paper making, nanocomposites, coating additives, security papers, food packaging, and gas barriers.

Although different studies have explored the use of PNB nanogels,[25−27] the synthesis of PNB in the presence of BC has been unexplored. The applications of hydrogels are usually limited due to their poor mechanical properties.[28] One possible

Received: December 20, 2012
Revised: March 1, 2013
Published: March 4, 2013

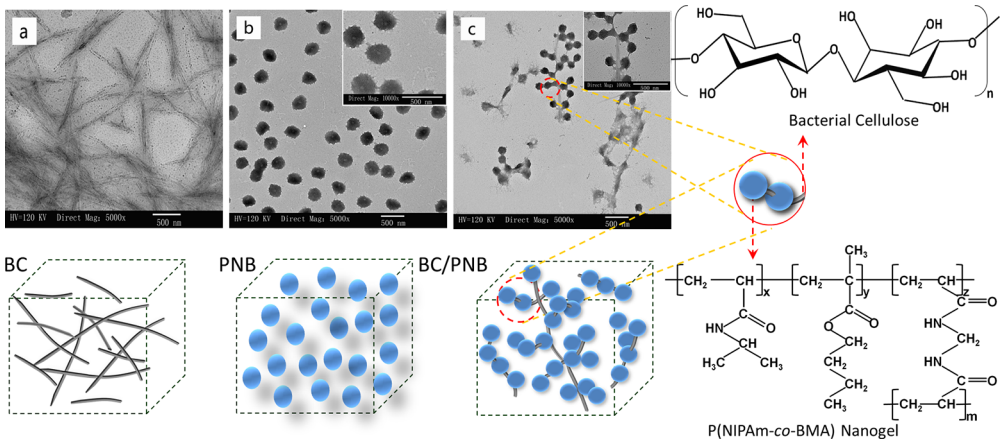

Figure 1. Morphology of BC/PNB nanogel complex: (a) TEM image for the BC whiskers; (b) TEM image for the PNB nanogel; (c) TEM image for the BC/PNB nanogel complex.

method for improving their structural design and thus their properties is through the preparation of compositions of BC and PNB nanogels. The present study focuses on the preparation of a biomaterial where PNB nanogels are synthesized in the presence of BC nanowhiskers to obtain a three-dimensional polymer network BC/PNB showing a shish-kebab morphology (Figure 1). Transmission electron microscopy (TEM), differential scanning calorimetry (DSC), and rheological investigations indicated that the formation of shish-kebab crystals, oriented molecular chains along the flow direction and well-developed spherulites are responsible for the observed improvements in mechanical properties.

The BC/PNB nanogel complexes create a new class of material that exhibit a wide range of control over the mechanical properties and the degree of anisotropy. By adjusting their composition and processing parameters, these nanogel complexes are suitable for soft tissue replacement applications, such as injectable materials. Previously, our group reported temperature-sensitive PNB nanogels as novel blood vessel embolic materials in the interventional therapy of liver tumors.[17] Temperature-sensitive PNB nanogels were synthesized, and their sol−gel phase transition was investigated. The study also reported that the PNB nanogel dispersion was miscible with iohexol (designated as PIB-I-6150). In the present study, BC whiskers were first prepared by hydrolysis with a mineral acid and then nanosized by high-pressure homogenization. They were subsequently utilized in the preparation of the BC/PNB nanogel complexes, which were expected to enhance the blood vessel embolization performance of the PNB nanogels. It was expected that a change in the topological structure of the nanomaterials would result in traumatic vascular endothelium formation, followed by endogenous coagulation and vascular thrombosis. The shish-kebab structures obtained through molecular design not only retained a low viscosity, shear thinning and fast sol−gel phase transitions, but also resulted in higher gel modulus. In addition to its application as a blood vessel embolic material, the BC/PNB nanogel complex can also be used as a restorative material for rapid filling of wounded tissue. We expect that BC could play a similar role as steel bars in concrete, by reinforcing the nanogel complexes to exhibit better mechanical strength.

MATERIALS AND METHODS

Materials. The wet BC membranes (95% humidity, consisting of a three-dimensional network of nano- and microfibrils of 10−200 nm width) used in this study were produced by Gluconacetobacter xylinus in our laboratory.[29] Concentrated sulfuric acid (98%, Tianjin Kermel) was used as received. *N*-Isopropyl-acrylamide (NIPAM, Acros) was recrystallized from *n*-hexane before use. Butyl methacrylate (BMA, Tianjin Kermel) was used as received. *N*,*N*′-Methylenebisacrylamide (MBAAm, Tianjin Kermel), employed as a cross-linker, was recrystallized from methanol. Sodium dodecyl sulfate (SDS) and other reagents were of analytical grade and used as received. Milli-Q ultrapure water was used in all the experiments.

Preparation and Characterization of Nano-Sized BC Whiskers. A BC emulsion containing nanocrystals was obtained by the sulfuric acid hydrolysis of BC wet membranes. This was followed by treatment in a high-shear homogenizer (FLUKO FA25−25F) for 15 min at a shear rate of 10000 rpm; the emulsion obtained was then characterized by TEM. The BC emulsion was freeze-dried and collected as a freeze-dried powder.

Preparation of PNB Nanogels and BC/PNB Nanogel Complexes. Pure PNB nanogels were synthesized according to a soap-free emulsion polymerization method reported in the literature;[30] they were identified as the N-0 group. The BC/PNB nanogel complexes were synthesized by adding freeze-dried BC powder to the emulsion polymerization process. Three different samples of BC/PNB nanogel complexes were synthesized for this study. They were labeled as the N-2, N-4, and N-6 groups, each containing a different percentage of BC whiskers, namely 10 wt %, 20 wt %, and 30 wt %, respectively. The dispersions obtained were lyophilized and collected as freeze-dried powders.

Nanogel Size and Morphology. The average diameter and zeta potential of the BC/PNB particles were measured on a Malvern Nano ZS 90 dynamic light scattering (DLS) instrument, with a He−Ne laser (633 nm) and a detection angle of 90°. The temperature-dependent diameter of the particles was also measured by DLS from 25 to 45 °C. The samples used for the measurements were nanogel dialysates, diluted with ultrapure water. All the samples were equilibrated for 2 min at the test temperature before the measurements. The morphology of the BC whiskers and BC/PNB at different temperatures was observed by TEM (JEM-1230, Japan) with an accelerating voltage of 200 kV. The BC/PNB nanogel dialysates were diluted with ultrapure water, and one drop of the solution was placed on a 400 mesh copper grid. After staining with 1% phosphotungstic acid, either of the copper grids was dried at 25 and 37 °C, for 2 h respectively.

Sol−Gel Transition Behavior of the BC/PNB Nanogel Complexes. The thermosensitive volume phase transitions of BC/PNB were evaluated by measuring the relative turbidity of aqueous dispersions of the nanogels at varying temperatures with a thermo-regulated UV/vis spectrometer. The wavelength used for the test was

dx.doi.org/10.1021/bm3019664 | *Biomacromolecules* 2013, 14, 1078−1084

625 nm, while the temperature was varied from 20 to 45 °C. The sample was maintained at the set temperature for 5 min before each measurement. A certain amount (0.05−0.25 g) of the lyophilized powder of N-0, N-2, N-4, and N-6 was weighed in four 5 mL plastic bottles, and then 1 mL of water was added to prepare nanogel dispersions at different concentrations. The four samples were left overnight at room temperature to swell fully, and then the "vial inversion with visual inspection" method was used to study the sol−gel transition behavior of the BC/PNB nanogel dispersions in the temperature range of 5−50 °C, with a precision of 0.1 °C.

Differential Scanning Calorimetry. The thermal properties of BC/PNB were measured with a Perkin-Elmer Jade DSC from 10 to 50 °C at a heating rate of 5 °C/min. Two samples for each formulation were analyzed to verify reproducibility.

Rheological Study of the BC/PNB Nanogel Complexes. The freeze-dried nanogel powder was dispersed in ultrapure water and maintained overnight at room temperature to generate aqueous nanogel dispersions (12 wt %). A strain-controlled rheometer (ARES 2000, TA) with parallel plate geometry (Φ = 40 mm) was used to measure the rheological properties of the aqueous nanogel dispersions.[31] The spacing of the parallel plates was set to 1 mm.

To perform the steady rate sweep tests, the shear rate-dependent viscosity (η) was measured at 25 °C and shear rates of 0.1−400 s^{-1}. To determine the linear viscoelastic region, a measurement was performed at a frequency of 1 Hz and 25 °C and percentage strains between 0.01 and 100%. The linear viscoelastic region was determined as the range where the dynamic rheological parameters (storage modulus G', loss modulus G'' and complex viscosity η^*) did not change with strain. Subsequently the temperature and time sweeps were performed within the linear viscoelastic region. The temperature sweep tests were conducted in the temperature range of 15−50 °C at a percentage strain of 0.1%, while the time sweep tests were conducted at a strain of 0.1% and a frequency of 1 Hz.

Biological Evaluation of BC/PNB Nanogel Complexes. Human umbilical vein endothelial cells (HUVECs) were maintained in Dulbecco minimal essential medium (DMEM), and supplemented with nonessential amino acids, L-glutamine, 10% fetal bovine serum (FBS), penicillin (100 U/mL), and streptomycin (100 U/mL). They were then seeded on a 96-well plate at a density of 10 000−20 000 cells/well. The BC/PNB nanogel complexes at concentrations of 0.01−50 mg/mL were assessed for their impact on the viability of the HUVEC cells by the MTT assay. Briefly, the nanogel complexes were successively diluted with DMEM and then incubated with the cells at 37 °C for 48 h. They were then replaced with 20 μL of MTT solution (5 mg/mL) and incubated for another 4 h. The crystallized product was dissolved in dimethyl sulfoxide (DMSO) and measured at 492 nm using a microplate reader. The cell viability index was calculated according to the following formula: Viability (%) = $(OD_{exp} - OD_{blank})/(OD_{control} - OD_{blank}) \times 100\%$. Four replicates were analyzed for each sample.

For the hemolysis measurements samples of the four groups, namely, the BC whisker/PNB nanogel complexes, the PNB nanogel, the sodium chloride injection (negative control), and the ultrapure water (positive control) were warmed in a water-bath at 37 °C until gelation occurred. Each group consisted of five 2 mL samples, which was supplemented with 2 mL of red blood cell suspensions. The samples were subsequently centrifuged at 4000 rpm for 5 min. The absorbance of the supernatant sample was measured at 540 nm to calculate the hemolysis rate according to the formula

$$\text{Hemolysis rate}(\%) = (\text{Abs}_{exp} - \text{Abs}_{\text{negative control}}) / (\text{Abs}_{\text{positive control}} - \text{Abs}_{\text{negative control}}) \times 100\%$$

RESULTS AND DISCUSSION

Morphology of the BC Whiskers and BC/PNB Nanogel Complexes. TEM images for the BC whiskers and the nanogel dispersions at 25 °C are shown in Figure 1. Isolated BC whiskers with a length of approximately 600 nm and diameters between 40 and 60 nm can be clearly observed (Figure 1a). At 25 °C the nanogels appeared as spheres with diameters of about 400 nm, while at 37 °C the nanogels shrunk and their diameter decreased to 150 nm. As seen in Figure 1c, BC whiskers were clearly visible among the PNB nanogels with nanogel particles gathering around the BC whiskers. This phenomenon may be attributed to hydrogen bonding between the hydrophilic hydroxyl groups of BC whiskers and the nanogel particles. Figure 2 shows the TEM images for the N-4

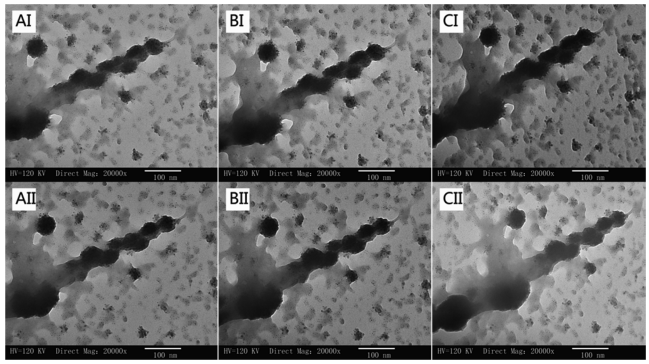

Figure 2. TEM images for the N-4 nanogel complex at 37 °C with tilt angles of 20° (AI), −20° (AII), 30° (BI), −30° (BII), 40° (CI), and −40° (CII), respectively.

BC/PNB nanogel complex with tilt angles of 20° (AI), −20° (AII), 30° (BI), −30° (BII), 40° (CI), and −40° (CII), respectively. It can be clearly identified that the BC whiskers act as a backbone stringing the PNB nanogel particles together, and the particles aggregate around the BC whiskers. The results further support our idea of the complexation of the nanogel spheres with nanocellulose.

Figure 3a shows the temperature dependence of the average diameter in the N-0, N-2, N-4, and N-6 dispersions. A narrow polydispersity index (PDI) (<0.1) was observed for all nanogel complexes with diameter of 350−450 nm. Evidently, the particle size of the four samples decreased with increasing temperature, and then leveled off. This is a typical behavior observed during the volume phase transition of nanogels based on PNIPAM.[32] A transition at approximately 30 °C was identified as the volume phase transition temperature (VPTT).[33]

The temperature dependence of the percent transmittance (T%) for diluted nanogel aqueous dispersion are shown in Figure 3(b). For all the nanogel systems an abrupt decrease in T% was observed when the temperature came close to 30 °C, indicating a sol−gel phase transition. As the temperature increased, a transition from swelling to contraction occurred in the nanogel systems, which resulted in an increase in the refractive index difference between the nanogel/water composite system and the water phase, producing a subsequent increase of turbidity. When the temperature exceeded the VPTT, the aggregation of nanogels also led to an obvious change in turbidity. These results indicate the temperature needed for the aggregation of nanogel particles.

The preparation of BC/PNB nanogel complexes utilized a physical blending process. Therefore, the sizes of the four nanogel complexes were independent of each other, and there was therefore no correlation between them. However, the large

dx.doi.org/10.1021/bm3019664 | Biomacromolecules 2013, 14, 1078−1084

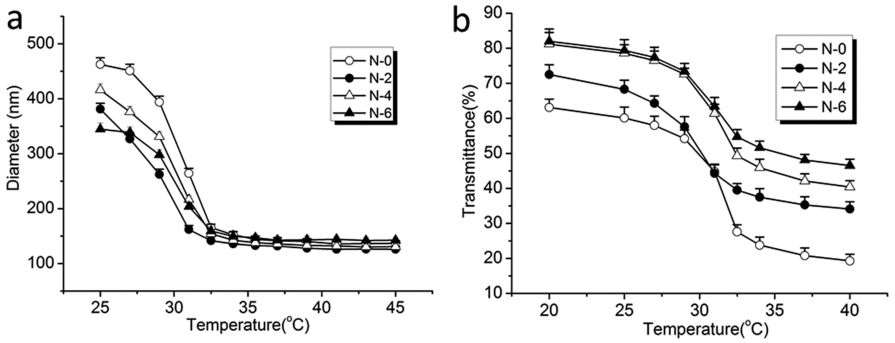

Figure 3. Temperature dependence of the size (a) and transmittance (b) of various BC/PNB nanogels: N-0(○), N-2(●), N-4(Δ), and N-6(▲). The concentration of all the nanogels was 0.5 mg·mL $^{-1}$.

number of hydroxyl groups on the BC whiskers strengthened the hydrogen bond interaction between hydroxyl groups and the crystal lattice water molecules in the BC/PNB nanogel system. As a result, the BC/PNB that had a higher content of BC would have attracted more water molecules around the BC/PNB nanogel complexes, resulting in a smaller refractive index difference between the nanogel/water composite system and the water phase, producing a higher transmittance. Therefore, the transmittance of nanogel dispersions increased with increasing amounts of BC whisker.

Thermosensitive Sol−Gel Phase Transition Behavior of the BC/PNB Nanogel Complexes. Nanogel dispersions of a certain concentration usually display four phases with increasing temperature (Figure 4). (1) At low temperatures, hydrogen bonding between water molecules and the nanogel particles is strong, making nanogel particles fully swollen. This is illustrated by the semitranslucent appearance of the swollen gel at macroscopic level. (2) With a rise in temperature, hydrogen bonding between nanogel particles becomes weaker, but partial hydrogen bonding between the water molecules and the nanogel particles is retained to give a translucent or transparent flowing nanogel suspension (clear suspension). (3) With a further rise in temperature, hydrogen bonding between the water molecules and the nanogel particles is destroyed, resulting in opaque turbid fluid at the macroscopic level (cloudy suspension). The temperature at which the transition takes place is called the cloud point temperature (CPT) or the VPTT. (4) As the temperature continues to rise, the number and strength of the hydrogen bonding interactions between the water molecules and the nanogel particles are further reduced, which leads to the formation of an opaque shrunken gel. Phase separation also occurs in the whole aqueous dispersion. The good fluidity at low temperature and the formation of a solid gel at high temperature by the nanogel aqueous dispersions could prove beneficial for applications in vascular embolization interventional therapy. Moreover, faster temperature response and lower viscosity compared with aqueous solutions of thermosensitive linear polymers could provide improved suitability for the transarterial embolization (TAE) treatment of hepatocellular carcinoma (HCC).[34,35]

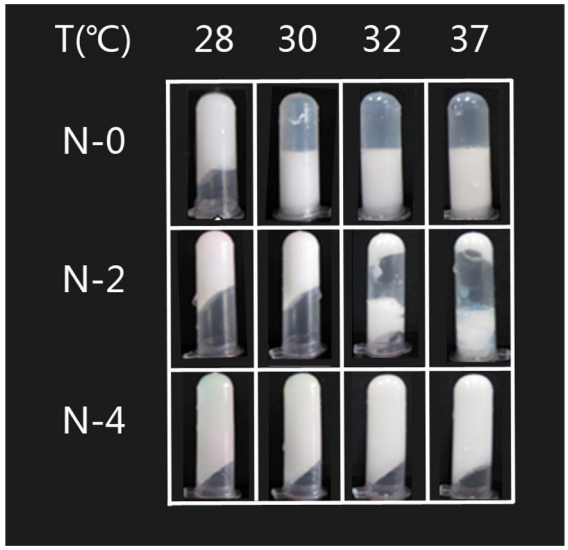

Figure 4. Illustration of the sol−gel transition of the BC/PNB nanogel complexes by the vial inversion and inspection method.

In this investigation, the visual inspection and dynamic viscoelastic methods were adopted to study the sol−gel phase transition of BC/PNB nanogels aqueous dispersions. The vial inversion method was applied for visual inspection of the sol−gel phase transition. It is a macroscopic observation for the sol−gel phase transition behavior of BC/PNB nanogels in a container, with flow corresponding to a sol and lack of flow corresponding to a gel. The dynamic viscoelastic method was also used for collecting relevant rheological datas for nanogel dispersions to characterize the sol−gel phase transition in order to avoid the possible subjectivity in the vial inversion method. As shown in Figure 4, the N-0 PNB nanogels and N-2 and N-4 groups of BC/PNB nanogel complexes underwent a sol−gel transition from a transparent fluid to an opaque precipitate as the temperature increased from 10 to 45 °C. Their corresponding VPTT were 30, 29.7, and 31 °C, respectively. The illustrations (Figure 4) indicate that a higher percentage content of BC whiskers in the BC/PNB nanogel complex correlates with a higher VPTT. Looking from top to bottom in Figure 4, the gels of nanogel complexes with a higher content of BC showed higher gel strength, whereas the gels with no or less BC showed instability and collapsed. This indicates that the addition of BC in the PNB nanogel enhances the gel strength at the macroscopic level, and higher BC content in the nanogel will result in a stronger gel. These results demonstrated the potential of using the BC/PNB nanogel complexes as an embolizing agent for interventional therapy of HCC, since embolizing agents with enhanced gelation strength are harder to remove.

Thermal Properties of the Thermosensitive Volume Phase Transitions of the BC/PNB Nanogel Complex. The thermal properties of the BC/PNB nanogel complexes were

investigated using DSC. Figure 5 shows the DSC thermograms for N-0, N-2, N-4, and N-6. A transition associated with a

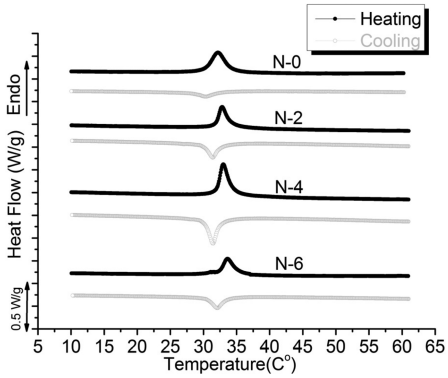

Figure 5. DSC thermograms for samples N-0, N-2, N-4, and N-6. The hollow symbols refer to a cooling scan, and the solid symbols refer to a heating scan.

LCST-type transition could be clearly identified at a heating rate of 5 °C/min. The phase transition peaks for N-0, N-2, N-4, and N-6 were at 32.2, 32.8, 33.0, and 33.3 °C, respectively. Judging from the DSC results combined with the rheological tests that will be discussed later, the onset temperature (T_t) was considered as the transition temperature because it represents the temperature at which the LCST transition begins. This transition was observed for all samples and appeared at an average temperature of $T_t = 31 \pm 1$ °C. It is important to emphasize that it is possible to shift the transition temperature to higher or lower values by adding new components to PNIPAM.[36] The PNB nanogel was polymerized using the following monomers: NIPAM (at 93.3 mol % of all monomers), MBAAm (at 1 mol %), SDS (at 0.5 mol %), potassium persulfate (KPS; at 0.2 mol %), and BMA (at 5 mol %). The hydrophobic poly(butyl methacrylate) (BMA) segment slightly lowered the VPTT of PNB nanogel in comparison to the PNIPAM nanogel, indicating that the variation of monomers in copolymerization had a significant effect on the volume-phase transition behavior.[12] Also, the increases of BC whiskers content in the four nanogel complexes led to an increase in the transition temperature. This is probably due to the large number of hydroxyl groups on the BC whiskers that could create hydrogen bonding with both water molecules and nanogel particles. This makes the nanogel network much more difficult to be destroyed, and therefore leads to a rise in the phase transition temperature. The endothermic peak appeared in the DSC thermograms corresponds to the energy absorbed to overcome the polymer−water interactions.

Rheological Properties of BC/PNB Nanogel Dispersions. Rheological analysis, an essential method for investigating the structure and characteristics of polymers, has been employed to study the viscoelastic behavior of the nanogel dispersions.[37] Figure 6 shows the steady shear viscosity (η^*) of the nanogels (N-0, N-2, N-4 and N-6) dispersed in water as a function of shear rate at 25 °C. The viscosity of the four nanogel dispersions decreased rapidly with increasing shear rate. This behavior is similar to pseudoplastic fluids, demonstrating shear thinning. The maximum viscosities of the N-2, N-4 and N-6 dispersions at room temperature were 400, 370, and 170 Pa·s, respectively, which is lower than that of

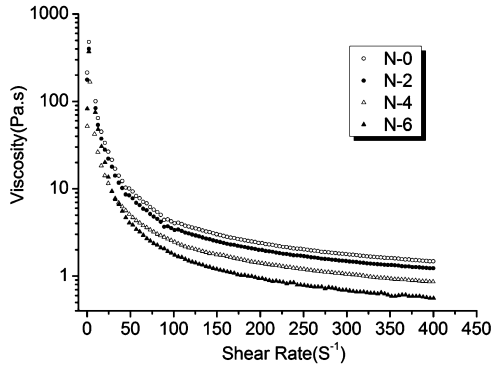

Figure 6. Shear rate dependence of viscosity η^* (Pa·s) of N-0, N-2, N-4, and N-6 nanogel complexes at 25 °C.

the PNB solution in all cases (ca. 790 Pa·s, at a concentration of 12 wt %). The lower viscosity of aqueous nanogel dispersions is an important property for application of injectable in situ gel-forming systems.

Figure 7 shows the dynamic temperature ramp cycle curves for N-0 and N-4 nanogel dispersions at a frequency of 1 Hz and a strain of 0.1%. With an increase in temperature, the rheological parameters (G', G'') first decreased and then increased remarkably. The decrease took place in a temperature range of 20−30 °C, which could be linked to the thermosensitivity of the nanogel particles. This decrease was followed by a large increase in G' and G'' as the temperature further increased, possibly due to an inherent characteristic of the nanogel dispersion.[38] Evidently, strong hydrogen bonding between the water molecules and the carbonyl and amid groups of the nanogel made the nanogel swell in water at low temperature. However, the water molecules were partially expelled from the nanogel as the temperature increased to 30 °C. This type of behavior is characteristic of entropy-driven hydrophobic interaction. It can therefore be assumed that the hydrophobic interactions from the isopropyl groups and the polymer backbone in PNB played a dominant role[39] and led to the collapse of the nanogel particles and gelation of the nanogel dispersion. The nanogel dispersion then became a shrunken gel, resulting in increased modulus and viscosity. At higher temperatures, G' and δ had the tendency to decline, possibly due to phase separation. In addition, Figure 7 shows that G' was always higher than G'', indicating that the elasticity was always dominant without the existence of a fluid state. This is because the high concentration (12 wt %) of the nanogel complex dispersion can lead to direct gelation from a semitranslucent swollen gel to a white shrunken gel with a rise in temperature. At 37 °C, the G' and G'' values for N-4 were respectively 500 and 57 Pa, while those for N-0 were 160 and 90 Pa. Obviously, a significantly higher G' was observed for N-4. This is most probably because of the large number of hydroxyl groups on the BC whisker surface that can increase the strength of hydrogen bonds between water molecules and BC/PNB nanogel system. Therefore, at the transition from fluid nanogel solution to solid gel at higher temperature, BC could reinforce the nanogel complexes to show higher mechanical strength, the same effect as steel bars in concrete. This rationale explains the significantly higher G' observed in N-4.

The curves also suggest that the sol−gel transition of the nanogel dispersions was reversible but with a clear hysteresis. This might be attributed to the shrunken compact structure of

dx.doi.org/10.1021/bm3019664 | Biomacromolecules 2013, 14, 1078−1084

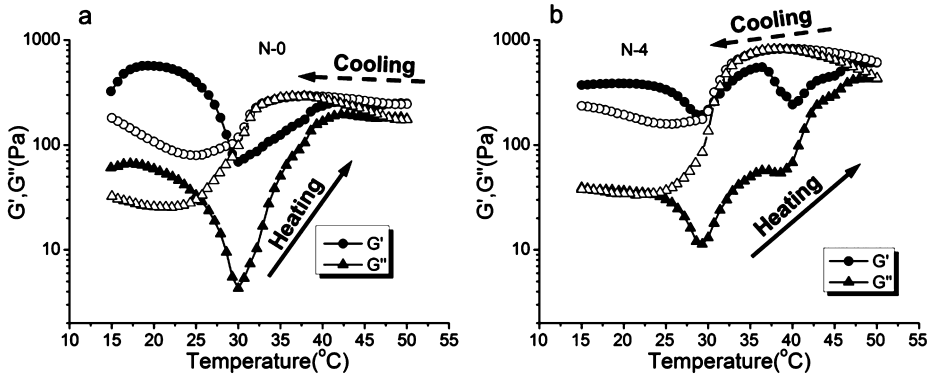

Figure 7. Dynamic temperature ramp cycle curves for N-0 (a) and N-4 (b) BC/PNB complexes aqueous dispersions. The hollow symbols refer to decreasing temperatures, while the solid symbols refer to increasing temperatures.

the particles in the nanogel at elevated temperatures that can block the surrounding water molecules from making the system swell again.

Biological Evaluation of BC/PNB Nanogel Complexes. PNB was shown to have low cytotoxicity in cell viability test after treatment with N-0 (without BC whiskers) (Figure 8).

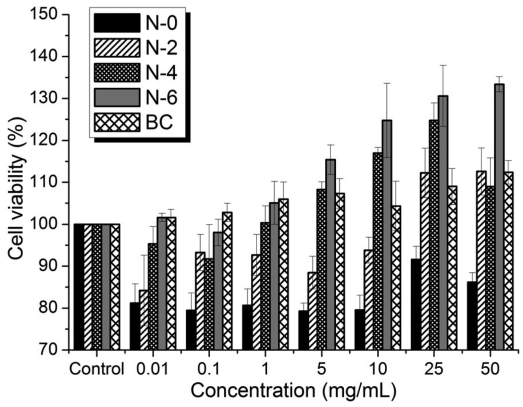

Figure 8. Relative growth rate (RGR) with BC whiskers and BC/PNB nanogels, respectively, at concentrations of 0.01−50 mg/mL as measured by the MTT test using HUVEC cells (n = 5). Incubation of the cells was performed at 37 °C.

The control group treated with BC whiskers slightly promoted the growth of HUVEC over the whole concentration range. Groups treated with N-2, N-4, and N-6, in which BC whiskers were combined with the nanogels at different concentrations ranging from 0.01 to 50 mg·mL^{-1}, showed a definite enhanced viability rate, which was even higher than that of the control group. We speculate that it is because the network structure of BC/PNB nanogel complexes formed by volume-phase transition is denser and tighter, causing the decrease of oxygen levels and resulting in a more pronounced expression of hemeoxygenase and cytoplasmic free Ca^{2+} concentration in HUVEC, followed by promotion of HUVEC proliferation.[40] This ability improved greatly as the concentration of BC whiskers increased.

Since a sodium chloride injection is considered to be completely biocompatible, the hemolysis rate of that negative control sample was set to zero. As shown in Table 1, the hemolysis rates for the PNB and BC/PNB complexes were 3% and 0.9%, respectively, which indicates that the BC/PNB nanogel complexes are more biocompatible than the PNB nanogels.

Table 1. OD Values and Hemolysis Rates for N-0 and N-4

samples	OD values (x ± s)	hemolysis rate (%)
positive control group	1.79 ± 0.09	100
negative control group	0.08 ± 0.01	0
experimental group 1 (N-0)	0.16 ± 0.01	3.0
experimental group 2 (N-6)	0.10 ± 0.01	0.9

CONCLUSIONS

BC/PNB nanogel complexes with different contents of BC whiskers were prepared by soap-free emulsion polymerization, and were identified to exhibit reversible thermosensitive phase behaviors with temperature changes. DLS and TEM characterization revealed that the nanogel complexes had an average size of about 400 nm at 25 °C and a narrow size distribution. In addition, the BC whiskers complexed well with the PNB nanogel particles, exhibiting shish-kebab morphologies. The concentrated nanogel complex dispersions showed good shear thinning behavior, which will prove beneficial for medical applications. The favored properties of easy flow at low temperatures and formation of solid gels at high temperatures make the BC/PNB nanogel aqueous dispersions an ideal injectable biomaterial and suitable for vascular embolization interventional therapy.

AUTHOR INFORMATION

Corresponding Author

*E-mail: yang_sunny@yahoo.com.

Notes

The authors declare no competing financial interest.

ACKNOWLEDGMENTS

The authors acknowledged the following funds and programs for financial support: the National Program on Key Basic Research Project of China (No. 2012CB932500), the National Natural Science Foundations of China (No. 21074041 and No. 50703014), the Natural Science of Hubei Province for Distinguished Young Scholars (No. 2008CDB279), and the Fundamental Research Funds for the Central Universities, HUST (No. 2010JC016). G.Y. thanks the China Scholarship Council for funding her as a senior visiting scholar to the University of Akron, U.S.A.

REFERENCES

(1) Saunders, B. R.; Vincent, B. *Adv. Colloid Interface Sci.* **1999**, *80*, 1−25.
(2) Morimoto, N.; Ohki, T.; Kurita, K.; Akiyoshi, K. *Macromol. Rapid Commun.* **2008**, *29*, 672−676.
(3) Jeong, B.; Kim, S. W.; Bae, Y. H. *Adv. Drug Delivery Rev.* **2002**, *54*, 37−51.
(4) Lee, C. C.; Gillies, E. R.; Fox, M. E.; Guillaudeu, S. J.; Frechet, J. M.; Dy, E. E.; Szoka, F. C. *Proc. Natl. Acad. Sci. U.S.A.* **2006**, *103*, 16649−16654.
(5) Ossipov, D. A.; Piskounova, S.; Hilborn, J. *Macromolecules* **2008**, *41*, 3971−3982.
(6) Blackburn, W. H.; Dickerson, E. B.; Smith, M. H.; McDonald, J. F.; Lyon, L. A. *Bioconjugate Chem.* **2009**, *20*, 960−968.
(7) Zhou, Y. M.; Ishikawa, A.; Okahashi, R.; Uchida, K.; Nemoto, Y.; Nakayama, M.; Nakayama, Y. *J. Controlled Release* **2007**, *123*, 239−246.
(8) Twaites, B. R.; de las Heras Alarcón, C.; Lavigne, M.; Saulnier, A.; Pennadam, S. S.; Cunliffe, D.; Górecki, D. C.; Alexander, C. *J. Controlled Release* **2005**, *108*, 472−483.
(9) Hong, S. W.; Kim, D. Y.; Lee, J. U.; Jo, W. H. *Macromolecules* **2009**, *42*, 2756−2761.
(10) Lee, E. S.; Kim, D.; Youn, Y. S.; Oh, K. T.; Bae, Y. H. *Angew. Chem., Int. Ed. Engl.* **2008**, *47*, 2418−2421.
(11) Aqil, A.; Vasseur, S.; Duguet, E.; Passirani, C.; Benoît, J. P.; Jérôme, R.; Jérôme, C. *J. Mater. Chem.* **2008**, *18*, 3352−3360.
(12) Zhao, Y.; Zheng, C.; Wang, Q.; Fang, J.; Zhou, G.; Zhao, H.; Yang, Y.; Xu, H.; Feng, G.; Yang, X. *Adv. Funct. Mater.* **2011**, *21*, 2035−2042.
(13) Gan, T.; Guan, Y.; Zhang, Y. *J. Mater. Chem.* **2010**, *20*, 5937−5944.
(14) Tai, H.; Wang, W.; Vermonden, T.; Heath, F.; Hennink, W. E.; Alexander, C.; Shakesheff, K. M.; Howdle, S. M. *Biomacromolecules* **2009**, *10*, 822−828.
(15) Hult, E. L.; Yamanaka, S.; Ishihara, M.; Sugiyama, J. *Carbohydr. Polym.* **2003**, *53*, 9−14.
(16) Bäckdahl, H.; Helenius, G.; Bodin, A.; Nannmark, U.; Johansson, B. R.; Risberg, B.; Gatenholm, P. *Biomaterials* **2006**, *27*, 2141−2149.
(17) Iguchi, M.; Yamanaka, S.; Budhiono, A. *J. Mater. Sci.* **2000**, *35*, 261−270.
(18) George, J.; Sajeevkumar, V.; Kumar, R.; Ramana, K.; Sabapathy, S.; Bawa, A. *J. Appl. Polym. Sci.* **2008**, *108*, 1845−1851.
(19) Helenius, G.; Bäckdahl, H.; Bodin, A.; Nannmark, U.; Gatenholm, P.; Risberg, B. *J. Biomed. Mater. Res., Part A* **2005**, *76*, 431−438.
(20) Klemm, D.; Kramer, F.; Moritz, S.; Lindström, T.; Ankerfors, M.; Gray, D.; Dorris, A. *Angew. Chem., Int. Ed.* **2011**, *50*, 5438−5466.
(21) Dong, X. M.; Kimura, T.; Revol, J. F.; Gray, D. G. *Langmuir* **1996**, *12*, 2076−2082.
(22) Araki, J.; Wada, M.; Kuga, S.; Okano, T. *Colloids Surf., A* **1998**, *142*, 75−82.
(23) Araki, J.; Wada, M.; Kuga, S.; Okano, T. *Langmuir* **2000**, *16*, 2413−2415.
(24) Edgar, C. D. In *223rd ACS National Meeting*, Orlando, FL, April 7−11, 2002; American Chemical Society: Washington, DC, 2002; p 116.
(25) Ruel-Gariépy, E.; Leroux, J. C. *Eur. J. Pharm. Biopharm.* **2004**, *58*, 409−426.
(26) Guilherme, M. R.; Campese, G. M.; Radovanovic, E.; Rubira, A. F.; Tambourgi, E. B.; Muniz, E. C. *J. Membr. Sci.* **2006**, *275*, 187−194.
(27) Pelton, R. *J. Colloid Interface Sci.* **2010**, *348*, 673−674.
(28) Coronado, R.; Pekerar, S.; Lorenzo, A. T.; Sabino, M. A. *Polym. Bull.* **2011**, *67*, 101−124.
(29) Klemm, D.; Schumann, D.; Udhardt, U.; Marsch, S. *Prog. Polym. Sci.* **2001**, *26*, 1561−1603.
(30) Serrano-Medina, A.; Cornejo-Bravo, J. M.; Licea-Claverie, A. *J. Colloid Interface Sci.* **2012**, *369*, 82−90.
(31) Hussain, S.; Keary, C.; Craig, D. *Polymer* **2002**, *43*, 5623−5628.
(32) Pelton, R. *Adv. Colloid Interface Sci.* **2000**, *85*, 1−33.
(33) Lee, B. H.; West, B.; McLemore, R.; Pauken, C.; Vernon, B. L. *Biomacromolecules* **2006**, *7*, 2059−2064.
(34) Stieger, M.; Richtering, W. *Macromolecules* **2003**, *36*, 8811−8818.
(35) Senff, H.; Richtering, W. *Colloid Polym. Sci.* **2000**, *278*, 830−840.
(36) Liu, W.; Zhang, B.; Lu, W. W.; Li, X.; Zhu, D.; De Yao, K.; Wang, Q.; Zhao, C.; Wang, C. *Biomaterials* **2004**, *25*, 3005−3012.
(37) Pal, R. *J. Colloid Interface Sci.* **2000**, *232*, 50−63.
(38) Wang, Q.; Xu, H.; Yang, X.; Yang, Y. *Polym. Eng. Sci.* **2009**, *49*, 177−181.
(39) Wu, J.; Huang, G.; Hu, Z. *Macromolecules* **2003**, *36*, 440−448.
(40) Schaefer, C. A.; Kuhlmann, C. R.; Weiterer, S.; Fehsecke, A.; Abdallah, Y.; Schaefer, C.; Schaefer, M. B.; Mayer, K.; Tillmanns, H.; Erdogan, A. *Atherosclerosis* **2006**, *185*, 290−296.